Scientific Research Publishing

Advances in Materials Physics and Chemistry, 2022, 12, 163-176
https://www.scirp.org/journal/ampc
ISSN Online: 2162-5328
ISSN Print: 2162-531X

Ag-Based Catalysts in Different Supports: Activity for Formaldehyde Oxidation

Rached Ousji[1], Zouhaier Ksibi[1], Abdelhamid Ghorbel[1], Céline Fontaine[2]

[1]Laboratory of Materials Chemistry and Catalysis, Faculty of Sciences of Tunis, University of Tunis El Manar, Tunis, Tunisia
[2]Institute of Chemistry of Poitiers: Materials and Natural Resources (IC2MP), University of Poitiers, Poitiers, France
Email: rached.ousji@fst.utm.tn

How to cite this paper: Ousji, R., Ksibi, Z., Ghorbel, A. and Fontaine, C. (2022) Ag-Based Catalysts in Different Supports: Activity for Formaldehyde Oxidation. *Advances in Materials Physics and Chemistry*, **12**, 163-176.
https://doi.org/10.4236/ampc.2022.128012

Received: June 26, 2022
Accepted: August 9, 2022
Published: August 12, 2022

Graphical Abstract

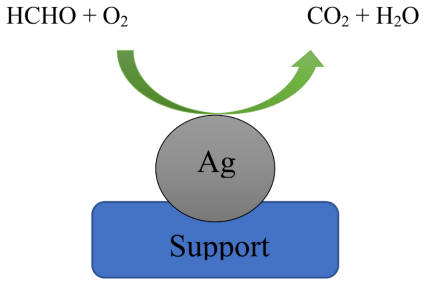

Abstract

Through the impregnation method, Ag catalysts with different support (such as TiO_2 and γ-Al_2O_3) were prepared and then tested for catalytic oxidation of formaldehyde (HCHO) at low temperatures. The Ag/TiO_2 catalyst exhibited strong catalytic performance, converting HCHO to CO_2 and H_2O at around 95˚C. However, the Ag/Al_2O_3 catalysts showed much lower activity and reached 100% conversion at 125˚C. The Ag-based catalysts were next characterized by several methods (XRD, TEM, FT-R, BET and H_2-TPR). Results of characterization revealed that support dramatically impacts the size and dispersion of Ag particles. The XRD analysis showed the existence of different peaks of the silver on the surface of Al_2O_3 in the contrast with TiO_2 no specific peaks exist. Therefore, the size of the Ag particles and their dispersion are the most important factors that affect their catalytic performance for formaldehyde oxidation. In terms of catalytic performance for HCHO oxidation, the Ag/TiO_2 catalyst possesses the best Ag dispersion, as well as the smallest Ag particle size.

Keywords

Formaldehyde Oxidation, TiO_2, Al_2O_3, Silver (Ag), Impregnation, Sol-Gel

1. Introduction

In the indoor environment, formaldehyde (HCHO) is a major source of indoor air pollution, which is harmful to human health. Exposure to HCHO over a long period of time can cause irritation in the eyes, deficits in spatial memory, allergic reactions and even cancer. In response to the increasing concern about this hazard, huge efforts have been made to eliminate indoor HCHO. The pollution caused by HCHO can be eliminated via a variety of methods, but catalytic oxidation gas has proven to be the most promising [1].

There have been certain types of catalysts that showed higher catalytic activity for oxidizing HCHO. It has been shown that noble metals supported catalysts, such Pt/TiO_2 [2], $Pt–CeO_2/NAC$ [3], Pt/MnO_2 [4], Pt/AC [5], Pt/Ni_x/a-AlOOH [6], Pd/CeO_2 [7], Pd/SBA-15 [8], Pd/TiO_2 [9], Au/SiO_2 [10], Au/CeO_2 [11], Au/Fe_2O_3 [12], Au/Co-Ce/Al [13] are active at room temperature for complete oxidation of HCHO to CO_2 and H_2O. Then, the high price of Pt, Au and Pd prevents their wide application and encourages studies of supported Ag-based catalysts, although it has a much lower price, it still shows considerable efficiency for oxidizing HCHO at low temperature. Lei *et al.* [14] prepared Ag/CeO_2 nanosphere catalysts by a one-step hydrothermal method and it displayed 110˚C as the complete oxidation temperature. According to a recent study, Ag/TiO_2 [15] could catalyze the 100% conversion of HCHO at 95˚C. Using Ag/MnO_x-CeO_2 catalysts (Tang *et al.*, 2006 [16] [17]), it was found that HCHO could be transformed into harmless H_2O and CO_2 at a temperature below 100˚C. In order to promote the catalytic activity of Ag-based catalysts, some factors have been investigated, including support, additives, and active oxygen species. For the oxidation of HCHO, Chen *et al.,* (2011) [18] compared the catalytic activity of Ag-based catalysts with different support. In their study, they found that Ag/MCM-41 displayed the best properties of all the catalysts, while the support played a significant role in catalytic activity. It was found that adding additives to Ag-based catalysts could enhance their catalytic activity. Bai and Li (2014) [19] found that the HCHO (100 ppm) removal efficiency increased to 55% at room temperature and 100% at 70˚C over a 1.7 %K-Ag/Co_3O_4 catalyst. In a recent study, Chen *et al.* (2017 [20]) found that single Ag could facilitate the activation of gaseous oxygen, thereby increasing the amount of active oxygen species that are beneficial to catalysis. The effect of pretreated condition investigated by Qin *et al.* (2017 [21]) is shown that the pretreatment condition of O_2 at 500˚C followed by H_2 at 300˚C has more effective catalytic activity on the oxidation of toluene over Ag/SBA-15 due to the small and highly dispersed Ag nanoparticles. However, Titanium oxide and alumina, used as a catalyst and support, have been of wide interest to scientists. Both supports present a very developed surface having acid-base sites and high mechanical and thermal stability, enabling a significant dispersion of active phases, which gives it exceptionally fascinating properties in heterogeneous catalysis. TiO_2 and Al_2O_3 can be synthesized by a variety of methods, including the sol-gel method. Sol-gel has the potential to produce different struc-

tures of materials such as bulk, fibers, sheets, films, and particles at low temperatures [22]. It makes conceivable both the creation of materials with high purity and homogeneity and additionally the control of particle-sized distributions at a nano-scale level [22]. In this paper, we prepared the Ag-based catalysts with supports of TiO_2 and Al_2O_3 by sol-gel and impregnation method, the silver content in the catalyst was 5% by weight, and then compared their performance for the catalytic oxidation of HCHO at low temperature. The catalysts are characterized by temperature-programmed reduction (TPR), X-ray diffraction (XRD), Brunauer-Emmett-Teller (BET), transmission electron microscope (TEM), fourier-transform infrared spectroscopy (FTIR) and their catalytic performance for HCHO oxidation was evaluated. The results were used to discuss and explain the activity of Ag-based catalysts.

2. Experimental

2.1. Preparation of Catalysts

All chemical reagents used to be of pure analytical grade. The TiO_2 with anatase structure and γ-Al_2O_3 powder were prepared by sol-gel method. Titanium (IV) isopropoxide ($Ti[OCH(CH_3)_2]_4$) formed a solution after 30 min of stirring absolute ethanol. Ethylacetoacetate (Eacac/Ti = 1, molar ratio) was added in the solution to control hydrolysis and condensation reaction rates. After 30 min of stirring an aqueous solution of nitric acid (HNO_3, 0,1 M) was introduced to the mix (HNO_3/Ti = 10, molar ratio), and stirring continued until a yellow gel formed. Then, the sample was dried, and the excess solvent was removed in an autoclave under the supercritical conditions, and calcined at 500˚C with ramping rate of $1^{\circ}C{\cdot}min^{-1}$ under a flow rate 30 mL/min of oxygen. The same steps were used to synthesize the Al_2O_3 with Aluminum-tri-sec-butoxide ($C_{12}H_{27}AlO_3$) and 1-butanol, the uncolored gel formed was dried in different condition and calcined at 600˚C. The supported catalysts Ag/Al_2O_3 and Ag/TiO_2 were prepared by impregnation with an aqueous solution of silver nitrate ($AgNO_3$).

2.2. Characterization of Catalyst

BET surface area, pore volume and pore diameter of all samples were obtained from N2 adsorption isotherms using an ASAP 2020 micromeritics analyzer.

X-ray diffraction (XRD) measurements of catalysts were measured by using PANalytical X'pert PRO MPD diffractometer with a CuKα1 radiation (λ = 1.54060 Å) and operated at 40 kV and 40 mA. The patterns were taken in the 2θ range of 10˚ - 70˚.

The programmed H_2 temperature reduction profiles (H_2–TPR) were carried out on chemisorption analyzer Autochem 2920 equipped with a TCD detector The TPR technique is based on the determination of hydrogen consumption for the reduction of metal oxides as a function of temperature. The temperature was in the range of 40˚C to 550˚C using a 5% H_2 /Ar gas mixture with a ramp of 5˚C/min and a flow rate of 30 ml/min.

Fourier transform infrared spectroscopy (FTIR) was used to identify types of molecular bonds in samples using the Perkin Elmer spectrometer. The samples were analyzed in the frequency range 400 - 4000 cm^{-1} with an irradiating source in the IR medium.

2.3. Measurement of Catalytic Activity

The source of formaldehyde used during the tests, therefore, comes from the dissolution of paraformaldehyde at 50˚C overnight with stirring. The activity tests for the catalytic oxidation of HCHO (100 ppm) over the Ag/Al_2O_3 and Ag/TiO_2 catalysts (50 mg) were performed with a fixed-bed quartz flow reactor by passing a mixture gas of 19.5% O_2, 78% N_2, and 2.5% H_2O balance at a total flow rate of 100 $cm^3 \cdot min^{-1}$, within the temperature range of 50˚C - 350˚C. After reaching the steady state, the effluent gas was analyzed (MKS Multigas 2030) for HCHO conversion and CO_2 selectivity. The HCHO conversion was calculated by this equation:

$$\text{HCHO Conversion}(\%) = \frac{[\text{HCHO}]_{in} - [\text{HCHO}]_{out}}{[\text{HCHO}]_{in}} * 100$$

where $[\text{HCHO}]_{in}$ and $[\text{HCHO}]_{out}$ are HCHO concentration at the inlet and outlet, respectively.

The apparent selectivity for carbon dioxide, are calculated as presented by the following equation:

$$(\text{Pi})\text{Selectivity}(\%) = \frac{[\text{Pi}]}{\sum[\text{Pj}]} * 100$$

where $[\text{Pi}]$ is the product concentration and $[\text{Pj}]$ is the sum of all reaction product concentrations.

The previous selectivity values will make it possible to calculate the yields of these products as shown on the equation:

$$(\text{Pi})\text{Yield}(\%) = \text{HCHO Conversion} * \text{S}(\text{Pi})$$

3. Results and Discussion

3.1. Catalytic Test

The catalytic activities and the selectivity of by-products, of pure supports (TiO_2 and Al_2O_3) and the catalysts (Ag/TiO_2 and Ag/Al_2O_3) were evaluated for the HCHO oxidation as shown in Figure 1. It is evident that the most efficient catalyst for HCHO oxidation was the Ag/TiO_2, while the worst active catalyst was pure Al_2O_3 the order of activity observed was Ag/TiO_2 >> Ag/Al_2O_3 > TiO_2 > Al_2O_3. To more understand the effect of support modification, the catalytic properties of TiO_2 and Al_2O_3 without silver were studied. The results obtained showed that the pure supports have an average activity, but cannot completely convert HCHO into CO_2 and H_2O. The main by-products found it in the outlet of gases is the CH_3OH and CO with a low selectivity of dioxide of carbon (CO_2).

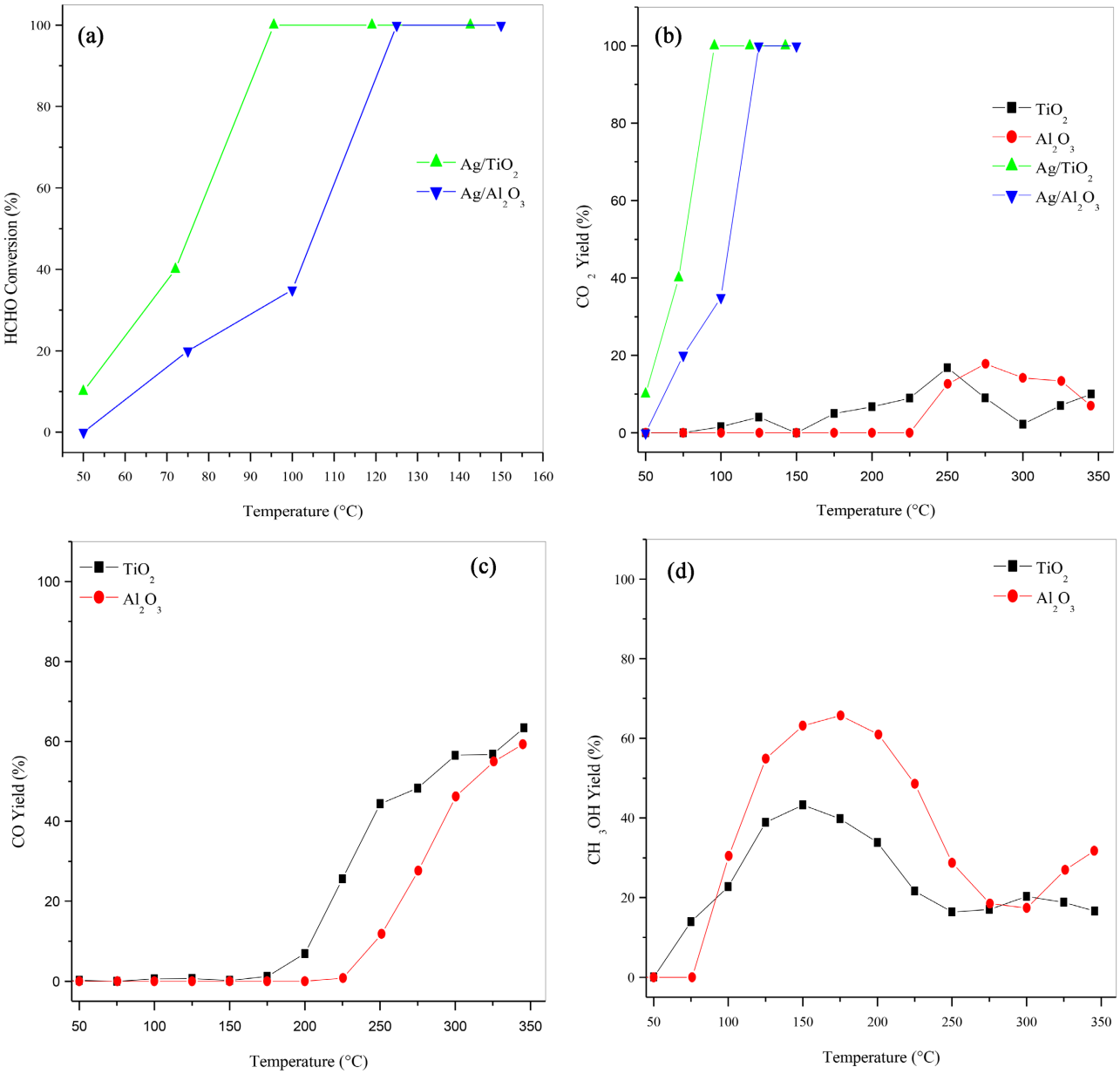

Figure 1. HCHO conversions (a), CO_2 yield (b), CO yield (c), CH_3OH yield (d) on TiO_2, Al_2O_3, Ag/TiO_2 and Ag/Al_2O_3. Reaction conditions: HCHO 100 ppm, catalyst mass 50 mg, O_2 19.5 vol%, total flow rate 100 $cm^3 \cdot min^{-1}$, GHSV 84,000 h^{-1}

Zhang and all [15] proved that TiO_2 and Al_2O_3 showed no activities for HCHO oxidation in the range of temperature 35˚C - 125˚C. The study of Hang and al [23] showed that TiO_2 and hydrogenated TiO_2 have a little activity after 200˚C. According to these data, the catalytic activity of the supports synthesized by sol-gel method is significantly important. Therefore, the supports modification by impregnation of silver on the surface, results in an increase of catalysts performance as well as the selectivity of formaldehyde oxidation to CO_2. The Ag/TiO_2 catalyst has better oxidation activity, the complete HCHO conversion to CO_2 is achieved at 95˚C. Total elimination of formaldehyde over Ag/Al_2O_3 catalyst is exhibited at 125˚C. We can conclude that the addition of Ag can pro-

vide sufficient active sites for the HCHO oxidation reaction. Note that the efficiency of the Ag/TiO_2 catalyst in the conversion of HCHO at low temperature (particularly T_{50}) is better than some literature data Table 1.

3.3. Characterization of the Catalysts

Figure 2 displays the XRD patterns of TiO_2 and Ag/TiO_2 catalysts. Diffraction peaks at 25.44˚, 38.0˚, 48.3˚, 54.43˚ and 63.4˚ correspond to (101), (004), (200), (105) and (204) and were well matched of tetragonal anatase TiO_2 (JCPDS 01-071-1166). The XRD pattern of Ag/TiO_2 showed an increase in peaks intensities with no additional peak related to the silver. These results showed that Ag

Table 1. Catalytic activity of silver-based catalysts in the HCHO oxidation.

Catalysts	Reactions conditions	T_{50} (˚C)	References
Ag/TiO_2	100 ppm HCHO, O_2 19.5 vol%, GHSV 84,000 h^{-1}	79	This work
Ag/CeO_2	810 ppm HCHO, O_2 20 vol%, 84,000 h^{-1} SV	90	[14]
Ag-HMO	400 ppm HCHO, 10 vol% O_2, 30,000 ml (gh) SV	80	[24]

With GHSV: gas hourly space velocity.

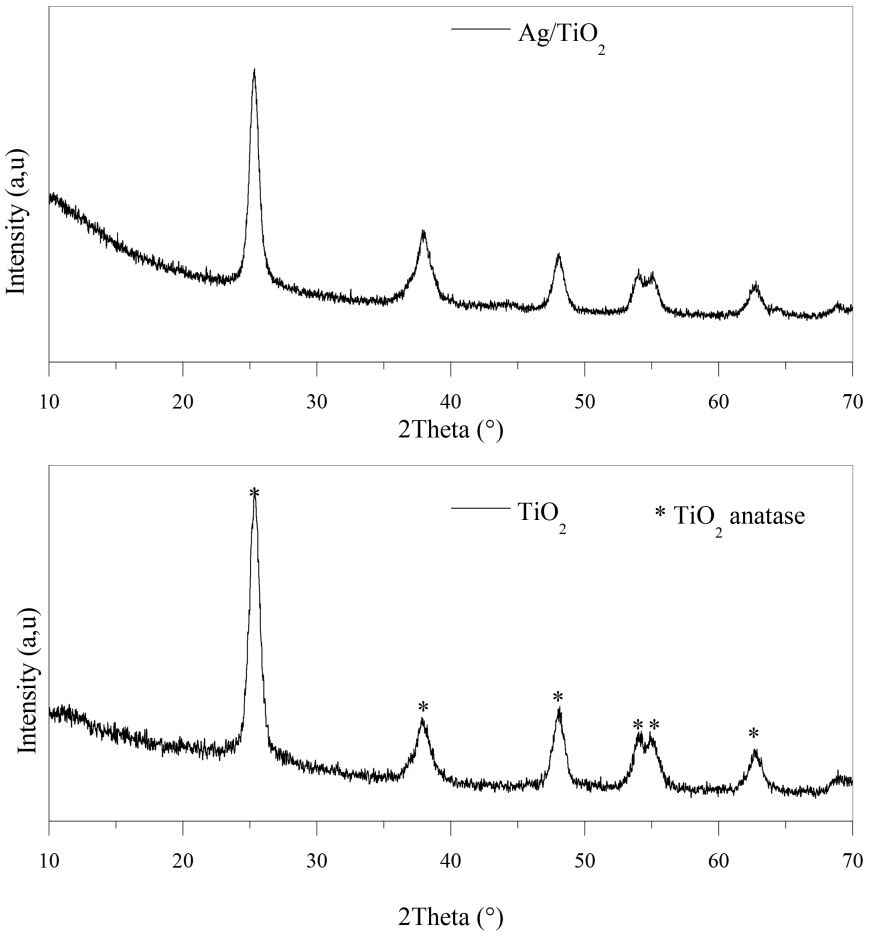

Figure 2. X-ray diffraction patterns of: TiO_2 and Ag/TiO_2.

species were widely dispersed on TiO_2 support that may have been caused by the strong interaction metal-support [25]. XRD patterns of Al_2O_3 and Ag/Al_2O_3 catalysts are shown in **Figure 3**. Only the phase γ-Al_2O_3 was detected Al_2O_3 [26]. As for the Ag/Al_2O_3 the diffraction peaks of Ag_2O at 38.2˚ and 64.5˚ were observed, which assigned as (111) and (220) crystal planes. In addition, a peak of Ag was detected at 44.3˚ corresponded to the (200) lattice plane, which could be indexed to face-centered cubic phase [27]. The crystallite sizes of the synthesized catalysts were calculated using the Debye-Scherrer equation and are presented in **Table 2**.

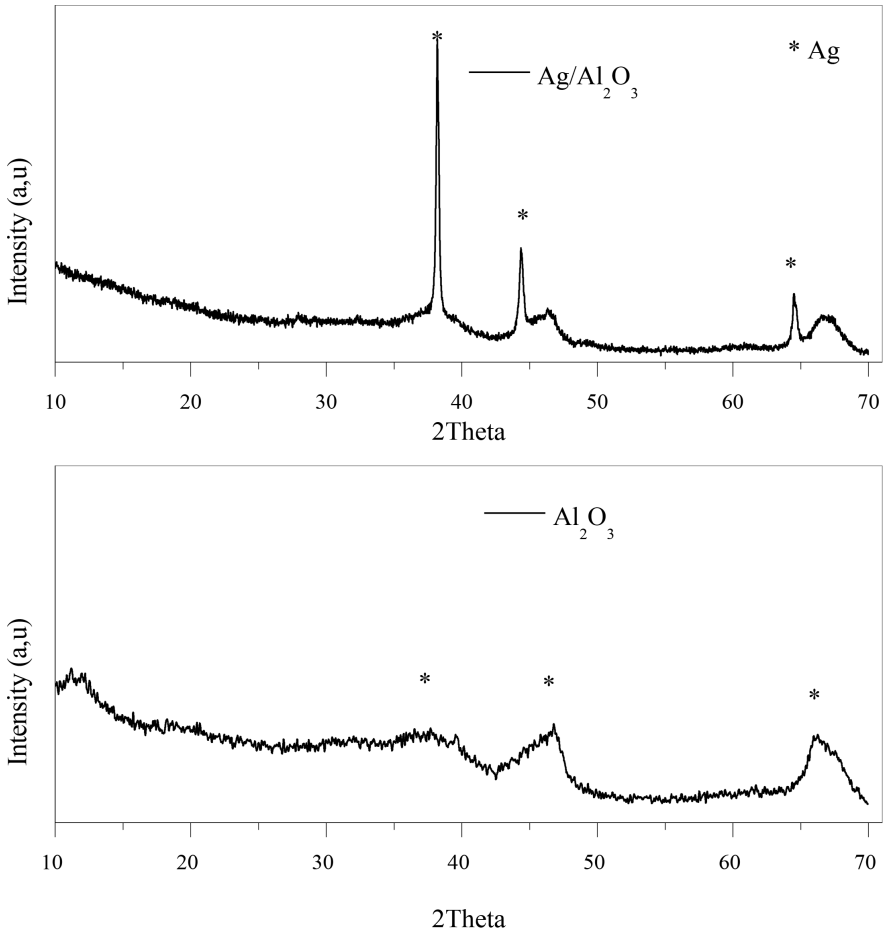

Figure 3. X-ray diffraction patterns of: Al_2O_3 and Ag/Al_2O_3.

Table 2. Material properties of synthesized catalysts.

Catalyst	S_{BET} (m^2/g)[a]	Pore volume (cm^3/g)[a]	Average pore diameter (Å)[a]	Crystal size (nm)[b]
TiO_2	132	0.38	84	-
Al_2O_3	322	0.69	62	-
Ag/Al_2O_3	247	0.40	59	25
Ag/TiO_2	104	0.28	77	14.6

[a]Determined by BET, [b]Determined by XRD.

The N_2 adsorption-desorption isotherms of Al_2O_3, Ag/Al_2O_3, TiO_2 and Ag/TiO_2 samples are presented in **Figure 4(a)** and **Figure 4(b)** show the isotherms of Al_2O_3 support and Ag/Al_2O_3 catalyst. Both solids belonged to type IV with a type H3 hysteresis, typically indicates the presence of closely packed slit pores [28]. As shown, in **Figure 4(b)** the isotherm of TiO_2 and Ag/TiO_2 samples resembled the type IV curves with H2 hysteresis loop, corresponding to mesoporous textures and in-bottle shaped. The Barrett-Joyner-Halenda (BJH) pore size distribution (**Figure 5(a)**, **Figure 5(b)**) Al_2O_3, Ag/Al_2O_3, TiO_2 and Ag/TiO_2 catalysts indicating that all samples characterized by a monomodal size distribution. The Brunauer-Emmett-Teller (BET) surface area, pore volume and average pore diameter obtained from N_2 adsorption-desorption measurement were showed in **Table 2**. The surface area of both TiO_2 and γ-Al_2O_3 supports gradually decreased after silver impregnation.

The optical analysis of FT-IR was used to determine the functional groups and vibration bonds in the samples in the range of 4000 - 400 cm^{-1}. **Figure 6** shows the FT-IR of Al_2O_3 support and Ag/ Al_2O_3 catalyst. The absorption peak at 3480 cm^{-1} is related to the vibration bonding of the hydroxyl groups OH. The peak of water molecules is formed at 1630 cm^{-1}. The vibrations peaks generated in the range of 700 - 500 cm^{-1} correspond to Al-O-Al, which proves the existence of γ-form [29]. **Figure 7** presents the FT-IR spectra of TiO_2 and Ag/TiO_2. The adsorption band in the range of 3800 - 3000 cm^{-1} are assigned to the stretching vibrations of OH. The peak absorption at 1620 cm^{-1} is ascribed to the adsorbed water molecules. The observed peaks at the range of 900 - 450 cm^{-1} is associated with the vibration of Ti-O-Ti [30] [31].

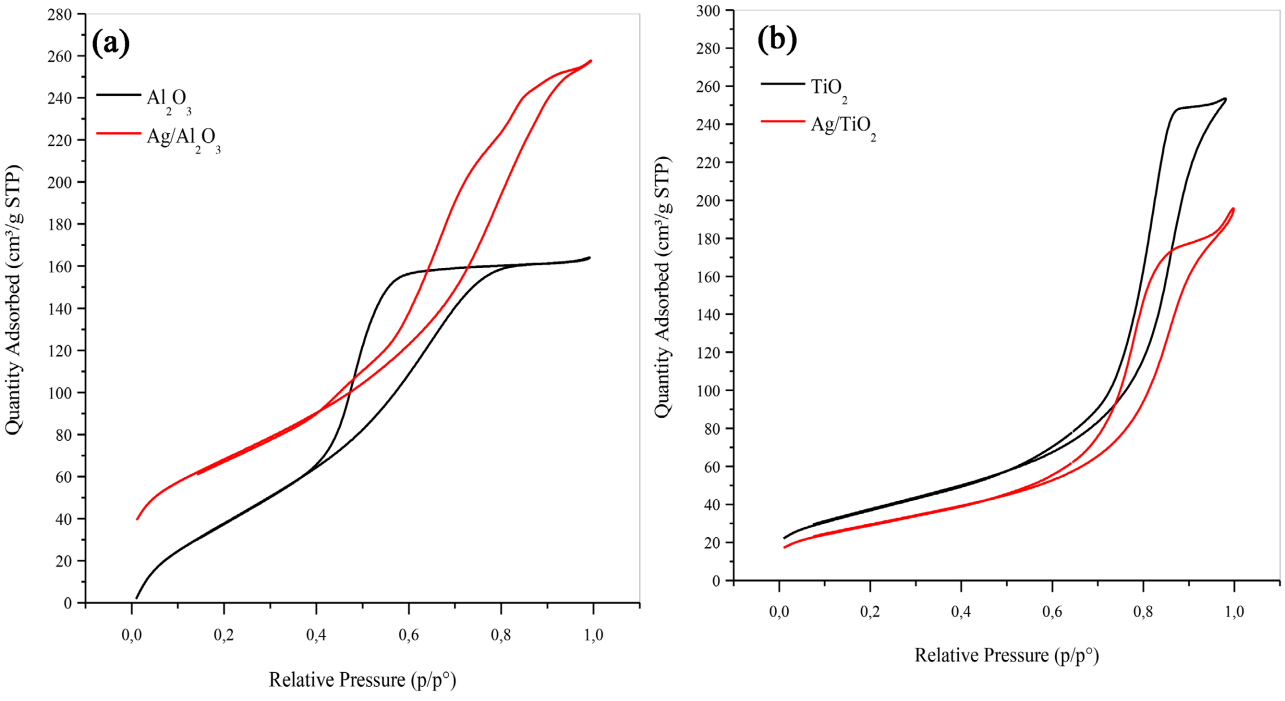

Figure 4. The curves of nitrogen adsorption-desorption isotherms of: Al_2O_3, Ag/Al_2O_3 (a) and TiO_2, Ag/TiO_2 (b).

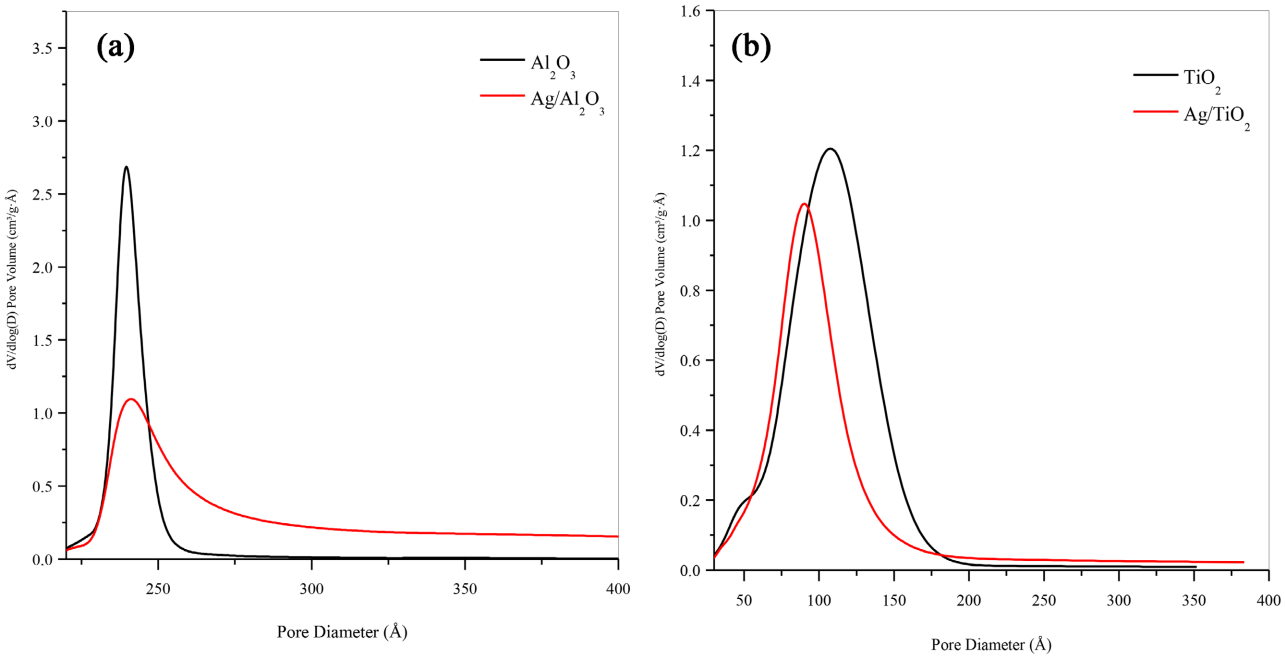

Figure 5. Pore size distribution curves of: Al_2O_3, Ag/Al_2O_3 (a) and TiO_2, Ag/TiO_2 (b).

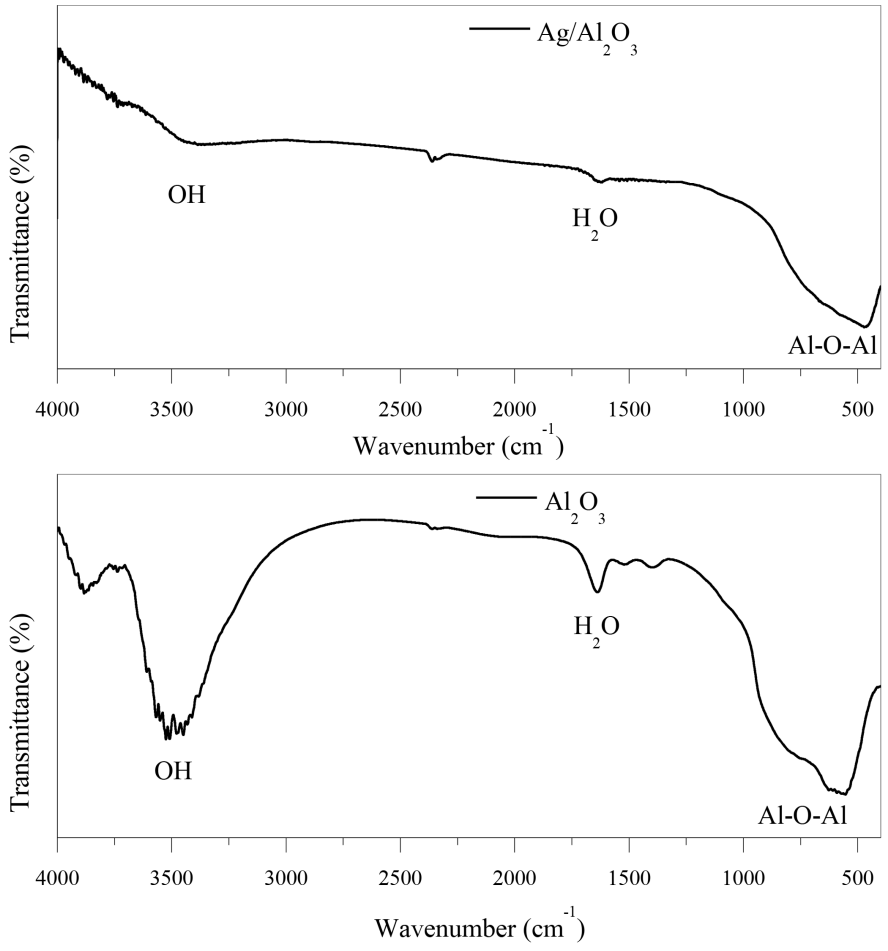

Figure 6. FT-IR spectrum of Al_2O_3 and Ag/Al_2O_3.

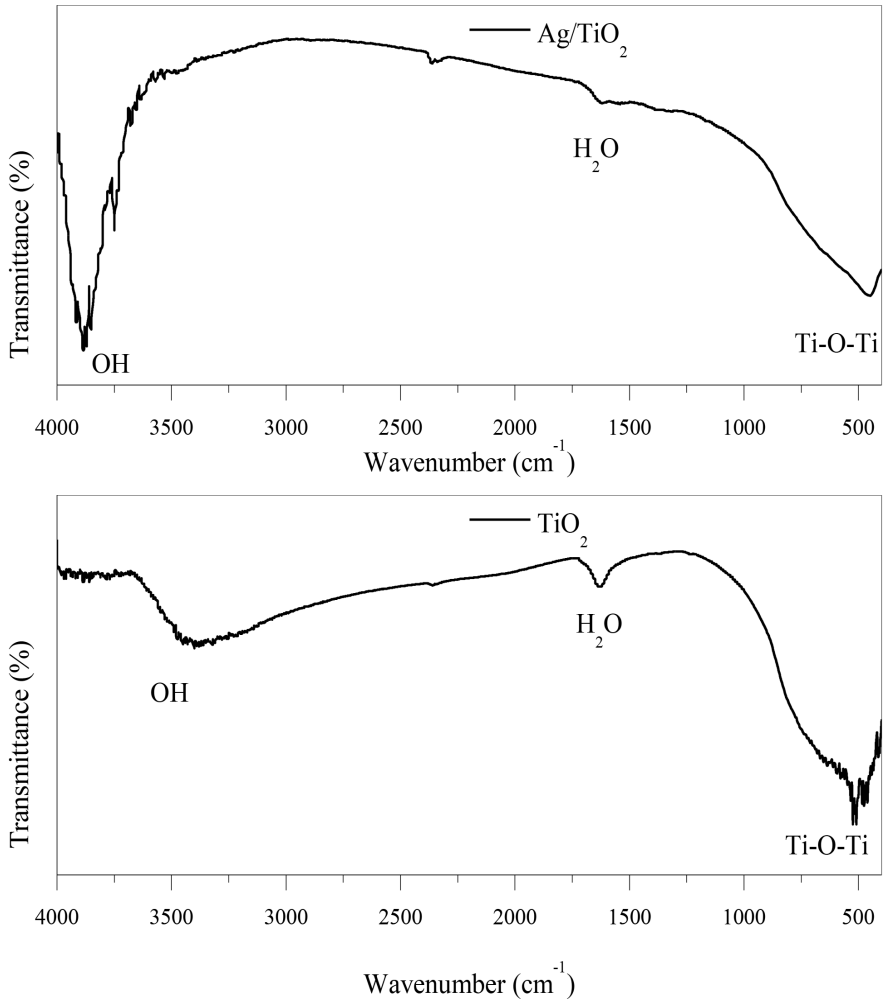

Figure 7. FT-IR spectrum of TiO_2 and Ag/TiO_2.

Transmission electron micrographs (TEM) of Ag/Al_2O_3 and Ag/TiO_2 catalysts are shown in **Figure 8** and **Figure 9**. The image of Ag/Al_2O_3 showed a distribution of Ag particles with nonuniform shapes, the silver present in the form of huge agglomerates composed of large particle sizes (**Table 1**). In contrast, in Ag/TiO_2 it can be observed that the Ag particle sizes are much smaller, and the distribution was relatively uniform. The addition of silver in the surface of TiO_2 support caused some black spots with a hexagonal structure. The results of TEM indicate that the impregnation of silver is very affected by the support used.

H_2-TPR experiments were conducted to investigate the redox ability of Ag/Al_2O_3 and Ag/TiO_2 catalysts and the results are shown in **Figure 10**. No reduction peaks observed in the profiles reported for the pure supports TiO_2 and γ-Al_2O_3. Two peaks were detected for Ag/Al_2O_3, peak around 100˚C caused by large Ag_2O clusters and the peak around 350˚C is assigned to small Ag_2O clusters [32]. For Ag/TiO_2 the peak below 100˚C was ascribed to reduction of oxygen species absorbed on the dispersed Ag surface, and the second peak was due to the reduction of large Ag_2O groups [27].

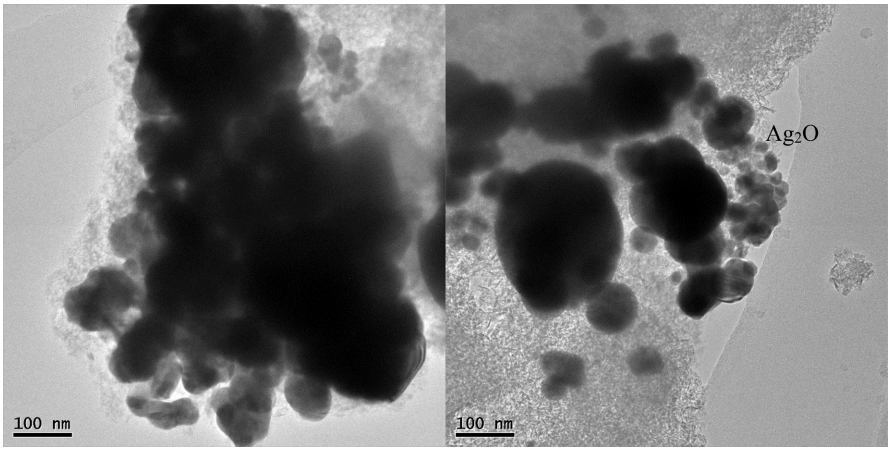

Figure 8. TEM images of Ag/Al_2O_3.

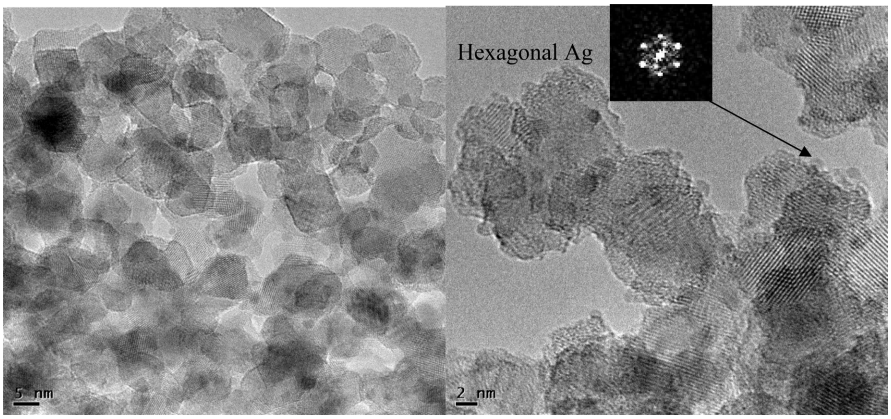

Figure 9. TEM images of Ag/TiO_2.

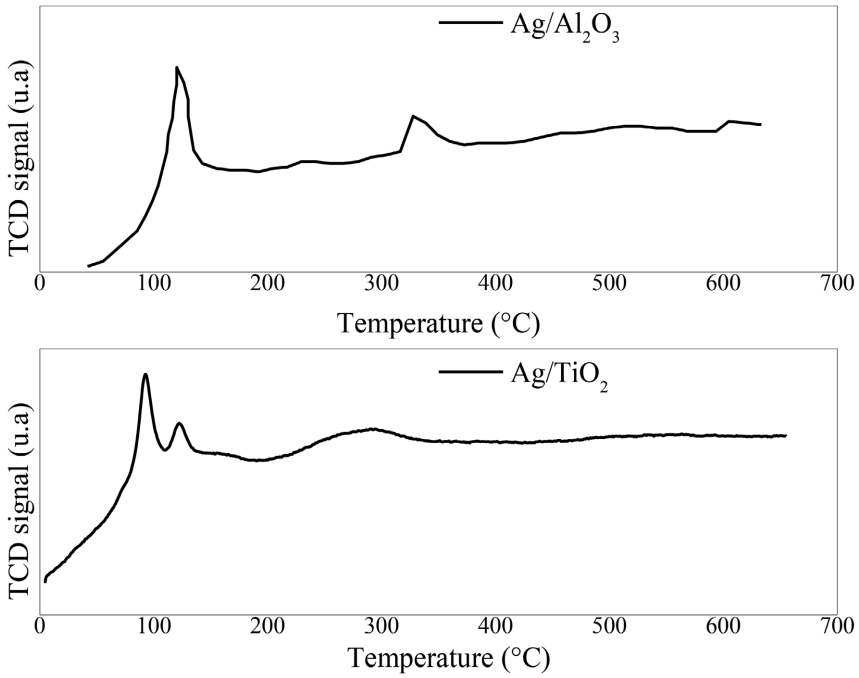

Figure 10. H_2-TPR profiles of Ag/Al_2O_3 and Ag/TiO_2 catalysts.

4. Conclusion

Ag/TiO_2 and Ag/Al_2O_3 were effective for the removal of formaldehyde (HCHO) leading to the selective production of carbon dioxide, unlike pure supports which release CO, and methanol as by-products. However, the activity of Ag/TiO_2 (100% conversion at 95˚C) was higher than Ag/Al_2O_3 (100% conversion at 125˚C). Characterization results indicated that Ag particle sizes and their dispersion in the surface of support are the important factors in the catalytic activity for formaldehyde oxidation. In summary, we have reported that the catalytic activity of supported Ag catalysts is dramatically influenced by the support morphology.

Author's Contributions

All authors conceived and designed the study. Ousji Rached conducted the experiments, analyzed the data and wrote the paper. All authors contributed to manuscript revisions. All authors approved the final version of the manuscript and agree to be held accountable for the content therein.

Conflicts of Interest

The authors declare no conflicts of interest regarding the publication of this paper.

References

[1] Bai, B.Y., Arandiyan, H. and Li, J.H. (2013) Comparison of the Performance for Oxidation of Formaldehyde on Nano-CO_3O_4, 2D-Co_3O_4, and 3D-CO_3O_4 Catalysts. *Applied Catalysis B*: *Environmental*, **142**-**143**, 677-683. https://doi.org/10.1016/j.apcatb.2013.05.056

[2] Su, Y., Ji, K., Xun, J., Zhang, K., Liu, P. and Zhao, L. (2021) Catalytic Oxidation of Low Concentration Formaldehyde over Pt/TiO_2 Catalyst. *Chinese Journal of Chemical Engineering*, **29**, 190-195. https://doi.org/10.1016/j.cjche.2020.04.024

[3] Bao, W., Chen, H., Wang, H., Zhang, R., Wei, Y. and Zheng, L. (2020) Pt Nanoparticles Supported on N/Ce-Doped Activated Carbon for the Catalytic Oxidation of Formaldehyde at Room Temperature. *ACS Applied Nano Materials*, **3**, 2614-2624. https://doi.org/10.1021/acsanm.0c00005

[4] Ye, J., Zhou, M., Le, Y., Cheng, B. and Yu, J. (2020) Three-Dimensional Carbon Foam Supported Pt/MnO_2 for Rapid Capture and Catalytic Oxidation of Formaldehyde at Room Temperature. *Applied Catalysis B*, **267**, Article ID: 118689. https://doi.org/10.1016/j.apcatb.2020.118689

[5] Wang, C., Li, Y., Zheng, L., Zhang, C., Wang, Y., Shan, W., Liu, F. and He, H. (2021) A Nonoxide Catalyst System Study: Alkali Metal-Promoted Pt/AC Catalyst for formaldehyde Oxidation at Ambient Temperature. *ACS Catalysis*, **11**, 456-465. https://doi.org/10.1021/acscatal.0c03196

[6] Zhao, S., Zhang, Q., Zhao, G. and Zhang, Y. (2020) Hydroxyl Enhanced Structured Pt/Nix/a-AlOOH Catalyst for Formaldehyde Oxidation at Room Temperature. *Modern Research in Catalysis*, **9**, 21-34. https://doi.org/10.4236/mrc.2020.92002

[7] Li, K., Ji, J., He, M. and Huang, H. (2020) Complete Oxidation of Formaldehyde over a Pd/CeO_2 Catalyst at Room Temperature: Tunable Active Oxygen Species

Content by Non-Thermal Plasma Activation. *Catalysis Science and Technology*, **10**, 6257-6265. https://doi.org/10.1039/D0CY01085E

[8] Xiang, N., Hou, Y., Han, X., Li, Y., Guo, Y., Liu, Y. and Huang, Z. (2019) Promoting Effect and Mechanism of Alkali Na on Pd/SBA-15 for Room Temperature Formaldehyde Catalytic Oxidation. *ChemCatChem*, **11**, 5098-5107. https://doi.org/10.1002/cctc.201901039

[9] Wang, C., Li, Y., Zhang, C., Chen, X., Liu, C., Weng, W., Shan, W. and He, H. (2021) A Simple Strategy to Improve Pd Dispersion and Enhance Pd/TiO_2 Catalytic Activity for Formaldehyde Oxidation: The Roles of Surface Defects. *Applied Catalysis B*: *Environmental*, **282**, Article ID: 119540. https://doi.org/10.1016/j.apcatb.2020.119540

[10] Chen, D., Shi, J. and Shen, H. (2020) High-Dispersed Catalysts of Core-Shell Structured Au@SiO_2 for Formaldehyde Catalytic Oxidation. *Chemical Engineering Journal*, **385**, Article ID: 123887. https://doi.org/10.1016/j.cej.2019.123887

[11] Bu, Y., Chen, Y., Jiang, G., Hou, X., Li, S. and Zhang, Z. (2020) Understanding of Au-CeO_2 Interface and Its Role in Catalytic Oxidation of Formaldehyde. *Applied Catalysis B*: *Environmental*, **260**, Article ID: 118138. https://doi.org/10.1016/j.apcatb.2019.118138

[12] Tang, Z., Zhang, W., Li, Y., Huang, Z., Guo, H., Wu, F. and Li, J. (2016) Gold Catalysts Supported on Nanosized Iron Oxide for Low-Temperature Oxidation of Carbon Monoxide and Formaldehyde. *Applied Surface Science*, **364**, 75-80. https://doi.org/10.1016/j.apsusc.2015.12.112

[13] Ilieva, L., Dimitrov, D., Kolentsova, E., Venezia, M.A., Karashanova, D., Avdeev, G., Petrova, P., State, R. and Tabakova, T. (2022) Gold-Based Catalysts for Complete Formaldehyde Oxidation: Insights into the Role of Support Composition. *Catalysts*, **12**, Article No. 705. https://doi.org/10.3390/catal12070705

[14] Ma, L., Wang, D., Li, J., Bai, B., Fu, L. and Li, Y. (2014) Ag/CeO_2 Nanospheres: Efficient Catalysts for Formaldehyde Oxidation. *Applied Catalysis B*: *Environmental*, **148**-**149**, 36-43. https://doi.org/10.1016/j.apcatb.2013.10.039

[15] Zhang, J., Li, Y., Zhang, Y., Chen, M., Wang, L., Zhang, C. and He, H. (2015) Effect of Support on the Activity of Ag-Based Catalysts for Formaldehyde Oxidation. *Scientific Reports*, **5**, Article No. 12950. https://doi.org/10.1038/srep12950

[16] Tang, X., Li, Y., Huang, X., Xu, Y., Zhu, H., Wang, J. and Shen, W. (2006) MnO_x-CeO_2 Mixed Oxide Catalysts for Complete Oxidation of Formaldehyde: Effect of Preparation Method and Calcination Temperature. *Applied Catalysis B*: *Environmental*, **62**, 265-273. https://doi.org/10.1016/j.apcatb.2005.08.004

[17] Tang, X., Li, Y., Chen, J., Li, Y. and Xu, Y. (2006) Complete Oxidation of Formaldehyde over Ag/MnO_x-CeO_2 Catalysts. *Chemical Engineering Journal*, **118**, 119-125. https://doi.org/10.1016/j.cej.2006.02.002

[18] Chen, D., Qu, Z., Shen, S., Li, X., Shi, Y., Wang, Y., Fu, Q. and Wu, J. (2011) Comparative Studies of Silver-Based Catalysts Supported on Different Supports for the Oxidation of Formaldehyde. *Catalysis Today*, **175**, 338-345. https://doi.org/10.1016/j.cattod.2011.03.059

[19] Bai, B. and Li, J. (2014) Positive Effects of K^+ Ions on Three-Dimensional Mesoporous Ag/Co_3O_4 Catalyst for HCHO Oxidation. *ACS Catalysis*, **4**, 2753-2762. https://doi.org/10.1021/cs5006663

[20] Chen, Y., Huang, Z., Zhou, M., Ma, Z., Chen, J. and Tang, X. (2017) Single Silver Adatoms on Nanostructured Manganese Oxide Surfaces: Boosting Oxygen Activation for Benzene Abatement. *Environmental Science & Technology*, **51**, 2304-2311.

https://doi.org/10.1021/acs.est.6b04340

[21] Qin, Y., Qu, Z., Dong, C. and Huang, N. (2017) Effect of Pretreatment Conditions on Catalytic Activity of Ag/SBA-15 Catalyst for Toluene Oxidation. *Chinese Journal of Catalysis*, **38**, 1603-1612. https://doi.org/10.1016/S1872-2067(17)62842-0

[22] Dimitriev, Y., Ivanova, Y. and Iordanova, R. (2008) History of Sol-Gel Science and Technology. *Journal of the University of Chemical Technology and Metallurgy*, **43**, 181-192.

[23] Chan, H.C, Chen, T., Xie, L., Shu, Y. and Gao, Q. (2018) Enhancing Formaldehyde Oxidation on Iridium Catalysts Using Hydrogenated TiO_2 Supports. *New Journal of Chemistry*, **42**, 18381-18387. https://doi.org/10.1039/C8NJ04472D

[24] Huang, Z., Gu, X., Cao, Q., Hu, P., Hao, J., Li, J. and Tang, X. (2012) Catalytically Active Single-Atom Sites Fabricated from Silver Particles. *Angewandte Chemie*, **124**, 4274-4279. https://doi.org/10.1002/ange.201109065

[25] Wang, F., Ma, J., He, G., Chen, M., Wang, S., Zhang, C. and He, H. (2018) Synergistic Effect of TiO_2-SiO_2 in Ag/Si-Ti Catalyst for the Selective Catalytic Oxidation of Ammonia. *Industrial & Engineering Chemistry Research*, **57**, 11903-11910. https://doi.org/10.1021/acs.iecr.8b02205

[26] Zhang, L., Zhang, C. and He, H. (2009) The Role of Silver Species on Ag/Al_2O_3 Catalysts for the Selective Catalytic Oxidation of Ammonia to Nitrogen. *Journal of Catalysis*, **261**, 101-109. https://doi.org/10.1016/j.jcat.2008.11.004

[27] Butovsky, E., Perelshtein, I. and Gedanken, A. (2012) Air Stable Core-Shell Multilayer Metallic Nanoparticles Synthesized by RAPET: fabrication, Characterization and Suggested Applications. *Journal of Materials Chemistry*, **22**, 15025-15030. https://doi.org/10.1039/c2jm32528d

[28] Wang, Y., Qu, Z., Xu, J. and Huang, B. (2020) Effect of Al_2O_3 Phase on the Catalytic Performance for HCHO Oxidation over Ag/Al_2O_3 Catalysts. *Applied Catalysis A. General*, **602**, Article ID: 117705. https://doi.org/10.1016/j.apcata.2020.117705

[29] Atrak, K., Ramazani, A. and Fardood, S.T. (2018) Green Synthesis of Amorphous and Gamma Aluminum Oxide Nanoparticles by Tragacanth Gel and Comparison of Their Photocatalytic Activity for the Degradation of Organic Dyes. *Journal of Materials Science: Materials in Electronics*, **29**, 8347-8353. https://doi.org/10.1007/s10854-018-8845-2

[30] Yu, J., Su, Y., Cheng, B. and Zhou, M. (2006) Effects of pH on the Microstructures and Photocatalytic Activity of *Mesoporous nanocrystalline titania* Powders Prepared via Hydrothermal Method. *Journal of Molecular Catalysis A: Chemical*, **258**, 104-112. https://doi.org/10.1016/j.molcata.2006.05.036

[31] Sakthivel, T., kumar, K.A., Ramanathan, R., Senthilselvan, J. and Jagannathan, K. (2017) Silver Doped TiO_2 Nano Crystallites for Dye-Sensitized Solar Cell (DSSC) Applications. *Materials Research Express*, **4**, Article ID: 126310. https://doi.org/10.1088/2053-1591/aa9e36

[32] Jabłońska, M., Nocuń, M. and Bidzinska, E. (2016) Silver-Alumina Catalysts for Low-Temperature Methanol Incineration. *Catalysis Letters*, **146**, 937-944. https://doi.org/10.1007/s10562-016-1713-x